J. Appl. Comput. Mech., 9(3) (2023) 870-883
DOI: 10.22055/jacm.2023.42249.3895

ISSN: 2383-4536
jacm.scu.ac.ir

Shahid Chamran University of Ahvaz

Journal of Applied and Computational Mechanics

Research Paper

Shape Optimization of Slotted Steel Plate Dampers using the Simulated Annealing Algorithm

Samuel Ferrer-Fuenmayor[1], Jesús D. Villalba-Morales[2]

[1] Departamento de Ingeniería Civil, Pontificia Universidad Javeriana, Cra 7 # 40-62, Bogotá, 1100-1000, Colombia, Email: ferrersamuel@javeriana.edu.co

[2] Departamento de Ingeniería Civil, Pontificia Universidad Javeriana, Cra 7 # 40-62, Bogotá, 1100-1000, Colombia, Email: jesus.villalba@javeriana.edu.co

Received November 03 2022; Revised December 17 2022; Accepted for publication February 02 2023.
Corresponding author: J.D. Villalba-Morales (jesus.villalba@javeriana.edu.co)

Abstract. This paper reports a procedure for maximizing the energy dissipation capacity (EDC) of a slotted steel plater damper by changing its initial geometrical shape. The methodology uses a simulated annealing algorithm to iteratively vary the slots' disposition, number, and geometry while improving the EDC. This capacity is computed for each tested configuration from a finite element analysis in ABAQUS, considering a cyclic displacement protocol. Five initial sections are enhanced, with the optimal one evoking a sand clock shape with two symmetric slots. The EDC increment is higher than 300%. It is observed that the objective function is multi-modal, and the optimal solution depends on the initial design. The proposed procedure is computationally easy to implement and requires less than fifty iterations to guarantee convergence in all cases.

Keywords: Metallic dampers, shape optimization, simulated annealing, slotted plates.

1. Introduction

The use of seismic protection devices (SPDs) in buildings has become a reality in several countries around the world (see reference [1]), representing an alternative to the conventional seismic design based on energy dissipation through the inelastic behavior of the structure. Introducing SPDs in a structure makes it possible to avoid the elements in the primary seismic force-resisting system suffering considerable damage in large earthquakes, increasing the structure's seismic performance and reducing the cost associated with repairs and loss of human lives. These devices can be classified into active, passive, hybrid, and semi-active devices according to the nature of their behavior [2]. Passive devices are preferred due to their low price; nonetheless, they cannot modify their properties in function of the seismic input. Japan presents more than 3000 buildings protected with seismic isolation, showing that the culture concerning the seismic hazard is essential [3]. In the United States, more than 350 structures have been equipped with buckling restrained braces since their introduction in the 1990s [4]. In addition, the company Quaketek has provided friction dampers for more than 50 structures worldwide in countries such as Canada, the United States, and Colombia [5]. There are many seismic protection devices; however, numerical and experimental research is being carried out to develop new devices that either reduce the seismic response during a seismic event or decrease their cost. It is worth mentioning that other strategies, such as self-centering devices, can efficiently minimize structural damage, as shown in [6].

A specific strategy to mitigate seismic damage in a structure consists of fuse elements that dissipate energy by concentrating inelastic displacements in hysteretic cycles. Different ways exist to use the movement during an earthquake to counter its effects, such as material yielding or friction. Typical Buckling Restrained Braces have a steel core with a yielding zone that concentrates the inelastic deformations in the element. A concrete cast guarantees that the performance of the braces is equal in compression and tension and the occurrence of stable cycles of hysteresis [7]. Friction dampers present a mechanism that dissipates energy through the sliding of two surfaces in contact due to the differential movement on each side supporting the damper; this happens after a pre-specified sliding force in the damper is achieved [8]. Metallic Yielding Dampers use inelastic displacements to generate energy dissipation in the whole device; one example is the triangle-added damping and stiffness (TADAS) damper [9]. Yielding could be raised by flexure, or shear stresses over the damper material. The design of a structure equipped with hysteretic-type dampers is ruled by international norms, such as ASCE 7-16 [10]. This code reports the experimental test required to guarantee the reliability of the devices, including the procedures to consider uncertainties in damper parameters in the structural analysis.

The slotted steel plate (SSP) dampers are configured for thin steel plates parallel to the beam. These dampers are hysteretic-type devices that dissipate energy when the steel yields due to the deformation introduced by the relative movements on the top and bottom of the devices (shear forces effect) during an earthquake. Experimental results on a cyclic test of individual specimens show that SSP dampers present regular and symmetric hysteresis cycles, even for large deformations [3]. This characteristic guarantees the reliability of the performance of the devices. However, research has shown that the dampers suffer a gradual strength reduction due to the beginning of flexural cracks in the slots' boundaries [11]. The use of SSP Dampers in structures has

Published online: February 12 2023

helped reduce their seismic response. Li et al. [12] reported levels of 90% in the reduction of the displacement of a reinforced concrete frame on the base floor when using a damper with an x-shape. Pimiento et al. [13] showed displacement reductions of up to 70% in a shaking table test of a three-story scaled steel frame using SSP dampers with circle and rectangle slots. Martinelli et al. [14] reported that low-cycle fatigue is a criterion that conditions the seismic response of a retrofit-reinforced concrete building. There is a high correlation between the top displacement and the seismic damage index of a structure. Teruna et al. [15] found that a trilinear approximation for the skeleton curve was adequate, being necessary to define two constants to describe the post-yielding behavior. On the other hand, the manufacture of this type of device is not complex and not expensive. Its installation on the structure is not complicated; therefore, they are very suitable for developing countries.

One of the aspects that influences the plates' energy dissipation capacity (EDC) corresponds to the shape, distribution, and quantity of slots. Chan et al. [5] found that the amount and distribution of circle slots influence the distribution of Von Mises Stresses through the plate and that the stress trajectory affects the zones where the yielding occurs. Zheng et al. [16] compared four distributions for vertical slots finding that this parameter affects the stability of the hysteretic cycles. Ferrer and Villalba [17] studied a set of plates with different shapes and found that the lowest and highest EDC difference could be up to 300%. Thus, it is possible to configure an optimization problem to determine the optimal topology for the damper to obtain the highest EDC from an available volume of steel material. Ghabraie et al. [2] optimized the shape of a rectangular slot through the BESO algorithm; they found an increment of up to 96% in the EDC. As a result, the stress distribution was improved. Xu et al. [18] optimized the boundary of honeycomb mild steel slit dampers by considering that each strip works as a bi-clamped beam under pure bending. Other research involving the optimization of metallic-yielding dampers were carried out by Watanabe et al. [19] and Deng et al. [9], obtaining the best position of stiffener elements in the damper. Both works showed that the optimal configuration for the damper presents a higher EDC. Liu and Shimoda [20] used Bezier Curves and an objective function based on the maximum cumulative equivalent plastic strain on both sides of the damper, with the constraint that the dissipated energy of the optimized shape is greater than the initial. Zhu et al. [21] compared two optimization criteria based on the *J2* Plasticity theory considering that all the points on the contour yield simultaneously, finding that the energy dissipation capacity increased between 40.65 and 63.69%. Farzampour et al. [22] used the Gray Wolf Algorithm to determine the optimal shape of butterfly-shaped shear links by maximizing the energy dissipation ratio by plastic deformation to the maximum equivalent plain strain.

The results above show that optimization is suitable for developing improved damper configurations. Notwithstanding, the selection of the optimization algorithm, either a heuristic or gradient approach, and the influence on the initial geometrical configuration of the damper are some issues that require further attention. This study presents a heuristic-based methodology for the shape optimization of SSP dampers based on maximizing the device's EDC, which can be applied to different initial shape dampers. The software ABAQUS is employed to compute the EDC of each shape tested under cyclic load. As this procedure presents a high computational cost, the Simulated Annealing Algorithm (SAA) is used to solve the optimization problem as it requires only one solution per iteration. Python is used to implement SAA and to get interaction with ABAQUS.

This research is significant because of the following reasons:

- It establishes a new shape for the SSP damper that presents the highest EDC for any given steel material quantity.
- It reduces the complexity in the computational implementation by using a free-of-derivatives algorithm, considering the interaction with Python and ABAQUS.
- It uses problem-knowledge heuristics to improve the convergence process.
- It assesses the influence of the SSP initial shape on the optimal result obtained by the optimization process.

2. Slotted Steel Plate Dampers

The working concept of such devices is quite simple; by introducing plastic deformations on Steel plates, it is possible to dissipate the seismic input energy. Different movement types could generate yield in the material, such as pure flexion, pure shear, and combined stresses. However, how the yielding is raised is not the only matter; it is essential to ensure that most of the device effectively yields and that the threshold of inducing deformation presents a minimum possible. The slotted steel dampers work mainly under shear stress, so they are formed by a thin perforated plate, such as the plate with vertical slots shown in Fig. 1a. It is possible to select several shapes for the slots, such as circles, triangles, or rectangles. Still, it is necessary to establish the optimum shape as the slots' shape, number, and position affect the sequence of how the strains will distribute on the plate. Figure 1b shows how the plate is installed into the structure with the thickness located perpendicular to the beam. The upper side is connected to the beam, while the lower side is connected to braces in a Chevron Configuration. Such configuration eases the relative strain between the device's top and bottom, inducing shear stress in the damper. However, it is necessary to guarantee that the plate does not present buckling perpendicular to the beam, reducing the device's effectiveness. There are different stiffener types to avoid out-plane buckling, such as the device proposed by Deng et al. [23]. The design of the primary seismic-force resisting system and the energy dissipation system have to guarantee that the SSP dampers yield first than the structural elements, as shown in the methodology proposed by Oviedo et al. [24]. It is worth accounting that the device and its connected components increase the structure's stiffness; thus, it could increase the shear force on the building. The attractiveness of using these devices is their manufacturing simplicity, low cost, and the possibility of being easily replaced after an earthquake (it works as a fuse).

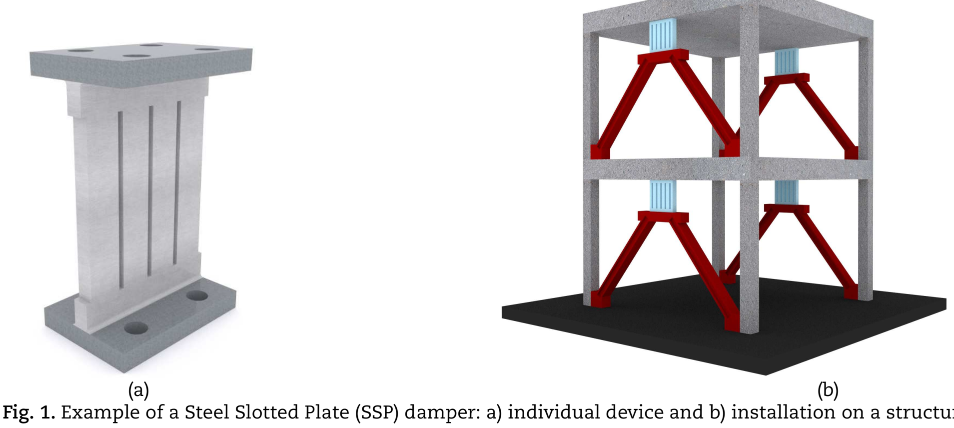

(a) (b)

Fig. 1. Example of a Steel Slotted Plate (SSP) damper: a) individual device and b) installation on a structure.

Different metallic materials can dissipate energy, such as steel and aluminum. Most papers deal with A-36 steel due to its yielding properties: low-yielding point and ductility. Yongjiu et al. [25] carried out a cycle test on A-36 steel specimens of 200 mm length, finding that the failure mode at a macro level corresponds to the contribution of the central region, buckling, and fracture; with a ductile failure in a micro level. However, researchers explore low-yielding point steels to decrease the device's deformation level to start dissipating energy [26]. Concerning the failure mode, it is observed that low-cycle fatigue can occur in high-stress concentration points. Jie et al. [27] experimentally show large deformations in the edges of slots due to the high stress in this zone raised in the shape of the damper. Perri et al. [28] showed that different steel types could present fatigue in different load cycles, observing that the area of the hysteretic process reduces in the cycle next to failure. Bae et al. [29] observed that including plastic hinges into a radius-cut coke-shaped strip damper resulted in higher ductility. Under the above findings, the challenge in numerical modeling is reproducing the results. For example, the definition of the constitutive model is an open question. Recent research show that different models could be adequate from experimental results [30]: Bilinear with isotropic hardening, Bilinear with kinematic hardening, trilinear, and Chaboche model.

To assess the ability of an SSP damper to dissipate energy is necessary to carry out a pseudo-cyclic test that introduces cyclic displacements in the upper surface of the damper while the bottom part is fixed. By doing that, it is possible to induce shear stress using load cycles established according to the protocols of documents such as EN-15129, ASCE 7-16 chapter 18, or FEMA 751. These documents also report how to include results coming from several tests. It is worth mentioning that the test of a device causes it to yield; therefore, it cannot be used in any building after testing. Furthermore, numerical integration on displacement and force measurements is used to compute the EDC. From a numerical point of view, this is possible by integrating the stress vector (f) and the displacement field (u) on the whole plate domain, as given by

$$E_p = \int f \times du \tag{1}$$

On the other hand, the following questions have to be raised when using SSP dampers: How will strains be induced in the device from their connection to the primary structural system? What shape will the slots of the device and outer edge have? What type of steel can be used? How can the device's performance to reduce the seismic response be computed? What are the protocols for the experimental test of the devices? What is the reliability of their performance under low-cycle fatigue? Which constitutive model will be used in the numerical model? There is no consensus in the literature on some of these aspects; a more detailed study is necessary to collect the current knowledge to address the main path to follow. A comprehensive state-of-the-art on hysteretic steel dampers can be found in the paper by Javanmardi et al. [31]. The present research has only a numerical phase; thus, the decisions on the above questions were taken from the literature.

3. The Simulated Annealing Algorithm

The Simulated Annealing Algorithm (SAA) is a stochastic heuristic method to solve search problems developed by Kirkpatrick et al. [32]. The algorithm follows an analogy of the principle of annealing metal materials that associates the best solution for an optimization problem with that state of the material without imperfections. Material perfection is achieved by slowly reducing the temperature to a lower energy state. Thus, a single solution is modified around its current neighborhood to generate better solutions and guide the search process. The main issue with SAA is the possibility that the algorithm will advance to a worse system state to prevent stagnation.

Figure 2 presents a typical flowchart for applying the SAA to solve an optimization problem defined by the objective functions, design variables, and constraints. The algorithm starts the iterative process by defining a single solution vector named design solution, randomly generated from the allowed values for each variable in the problem. First, the user must provide an initial value for the temperature parameter (T), which ranges from 0 to 1. The parameter determines if a trial solution is accepted as the design solution. Then, the trial solution is generated from a probabilistic expression that modifies the design solution inside a close space. Then, the objective function is computed, and the acceptance criterion is applied. The criterion compares a 0-1 random number against the acceptance probability (P), which is given by:

$$P(\Delta f, T) = e^{(\Delta f / T)} \tag{2}$$

where Δf is the difference between the quality of the trial and design solutions. High values of the temperature factor increase the probability that a trial solution is accepted even if it is worse than the current design solution. This characteristic is fundamental to avoid the algorithm getting stuck in local optimums. The trial solution becomes the design solution if the acceptance criterion is satisfied. The algorithm completes the process when a stop criterion is achieved, for example, when a maximum number of iterations is met. However, it is necessary to execute the algorithm in a predefined number of runs due to the stochastic nature of SAA.

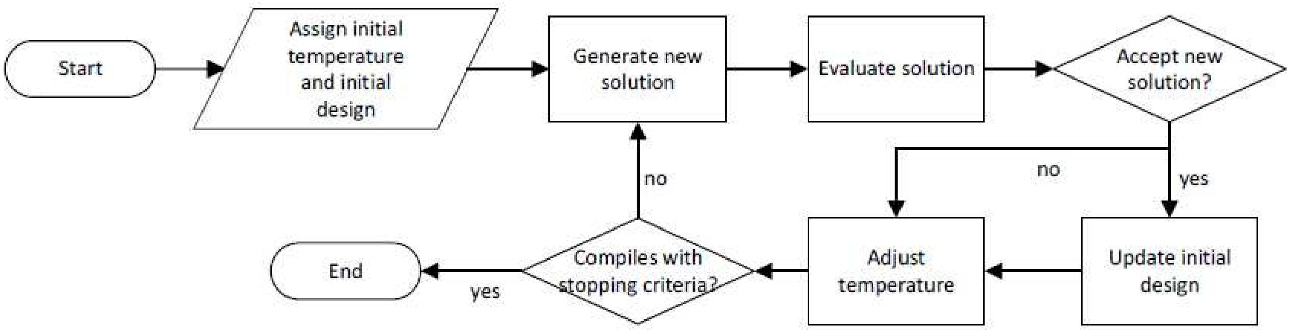

Fig. 2. Traditional Simulated Annealing Algorithm.

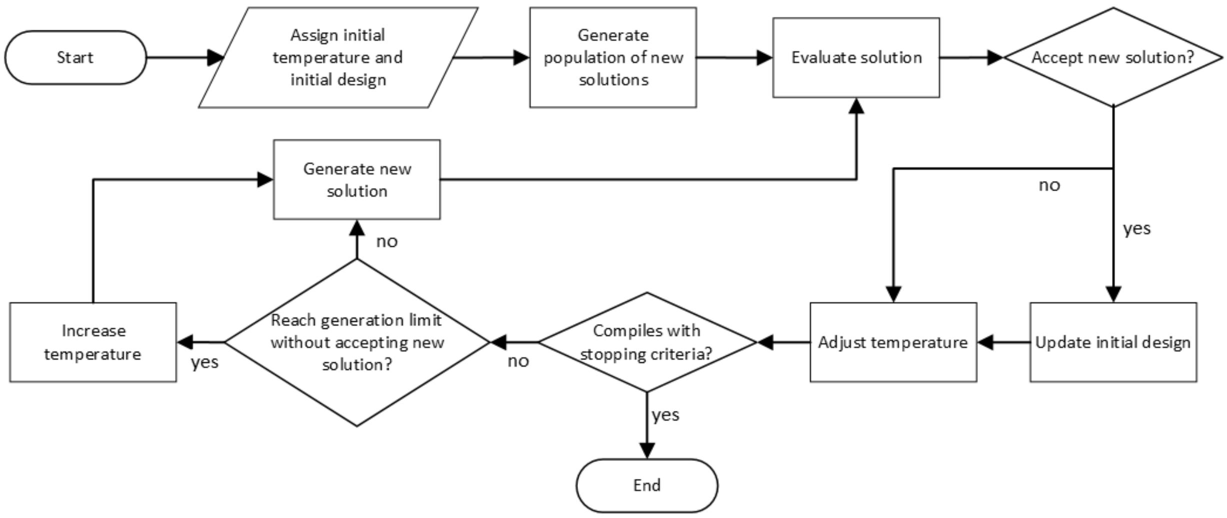

Fig. 3. Modified Simulated Annealing Algorithm [29].

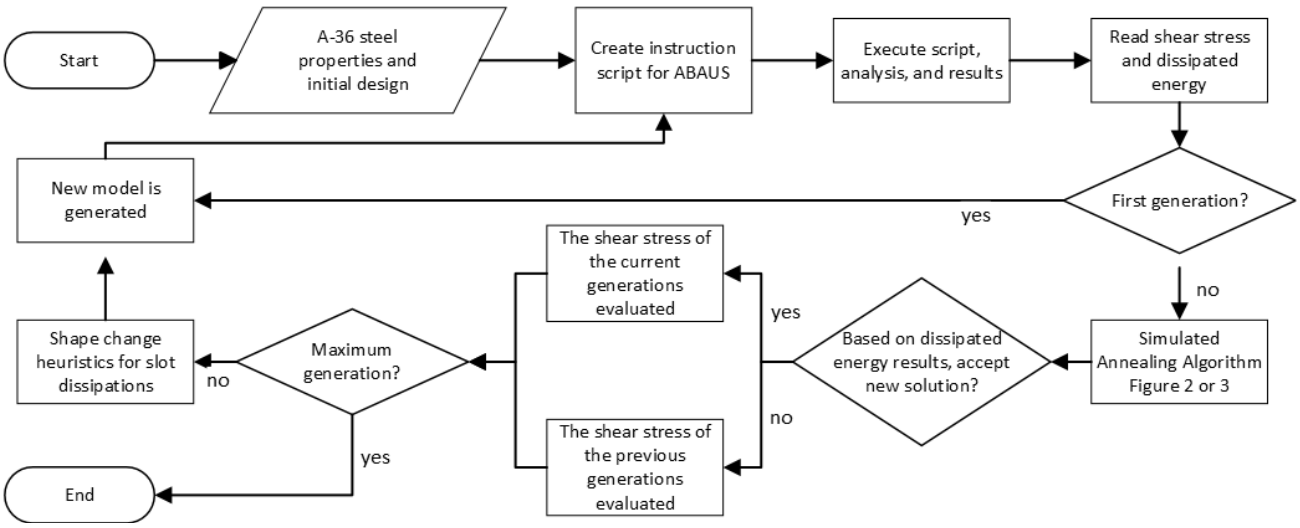

Fig. 4. Algorithm for the shape optimization of Slotted Steel Damper with a SAA and Abaqus.

Milan and Begambre [33] introduced three modifications to improve the performance of the SAA in terms of the final result and lower computational time. The first one is related to the fact that the current expression for the acceptance probability takes the algorithm more iterations to converge. In that sense, the following equation reduces half the probability of accepting a solution.

$$P(\Delta f,T)=\frac{1}{1+e^{(\Delta f,T)}} \tag{3}$$

The second modification decreases the dependence of the original SAA on the chosen initial design solution, as any other answer is a variation of that solution. Thus, the first trial SSP damper configuration corresponds to the highest objective function from a pool of randomly generated initial design solutions. Finally, the third modification introduces global exploration for high temperature and exploitation (local exploration) for low temperature by modifying the mutation factor used to generate the trial solution. The last modification considers that the mutation factor can change but in the function of the temperature factor. If the algorithm detects that it could be stuck in a local optimum, then the temperature will go up with the mutation factor to increase the ability to explore the search space. Figure 3 shows the flowchart for the modified SAA (MSAA) considering the above changes, as in reference [33].

It is worth mentioning that no metaheuristic method can efficiently solve all the optimization problems. Still, the SAA has proven its capability to solve different structural engineering problems. Some of these problems correspond to structural damage detection [34], structural size optimization [35], the optimal location of viscous dampers [36], and the optimal position of sensors for modal identification [37]. The necessity for adjusting SAA to the characteristics of each problem implies that the user has to know how to modify the computational implementation.

4. The Proposed Methodology for the Optimization of Slotted Steel Dampers

This research proposes a methodology to obtain the optimal shape for an SSP damper (see Fig. 1) that maximizes the dissipation energy capacity under cyclic load given a specific quantity of material in a predefined initial shape. The flowchart to apply the methodology is presented in Fig. 4. It is based on the interaction among finite element modeling software, the mathematical function of the optimization problem, and a search algorithm to solve the problem. It is necessary to carry out a dynamic non-linear finite element analysis for the plate suffering the cycles of seismic loads to determine its hysteretic behavior and later compute its EDC. In this case, the Software ABAQUS was used for numerical modeling. It allows the assessment of the plates' behavior under large deformations and the interaction among the different components of the algorithm. The mathematical formulation for the optimization problem is given in section 4.1 and requires to be implemented computationally, including some extra information derived from Abaqus. The optimization algorithm followed a heuristic approach as it facilitates introducing computational procedures to account for the problem knowledge (see section 4.3). The MSAA in Section 3 solved the optimization problem due to its convergence properties and a single-population algorithm. These characteristics are fundamentals to reduce the computational cost associated with applying the proposed methodology, as each possible solution tested implies one run of finite element analysis. The routines and the interaction with Abaqus were implemented in the programming language Python to assess the performance of the proposed methodology.

The search process of the device with the optimal shape is iterative, beginning from an initial plate configuration to obtain an enhanced plate in terms of its energy dissipation capacity. The user is faced with defining the quantity of material to manufacture the plate and its initial shape, which plays a crucial role in the optimal shape obtained. The MSAA could easily get trapped in a local optimum because the search space for the problem is multi-modal; this means that very different shapes for the plate can present similar values of the objective function to that of the global solution. Section 4.1 offers the computational representation for each damper. The steel used could also lightly affect the optimal shape, requiring an independent optimization process for each type. The results of this paper were obtained using a steel A-36, a common type of steel worldwide.

It is necessary to generate an Abaqus script to carry out the finite element modeling of the damper, as shown in Section 4.4. The modeling implies that the user has to provide the element type, the maximum size of the finite element mesh, constraints, constitutive model, type of analysis, load pattern, and desired results. The computational code executes the script in Abaqus, obtaining the time-history response of the plate to a predefined cycle load in terms of stresses and deformations. An additional code is implemented to compute the energy capacity dissipation of the damper.

The displacement cycle used to determine the plate's EDC was proposed by Ghabraie et al. [2] and carried out in four steps, as shown in Fig. 5. First, the plate starts from the position related to the initial configuration. Next, a displacement of 10 mm in the right top is applied, followed by a 20 mm displacement in the opposite direction, then the plate returns to its initial position. Finally, the lower side is kept restricted from movement. Such representations simulate the relative displacement between the support (on the damper's downside) and the beam (on the upper side). The superior boundary is only restricted in the vertical direction.

Then, the modified SAA in Section 3 is applied to the mathematical optimization problem defined in Section 4.1 after the user defines its parameters (see Section 4.2). A total of five trial plate shapes are derived from the initial design, with the trial solution being chosen as the plate with the larger EDC. The equations for generating the trial solutions are presented in Section 4.3. The algorithm is stopped when a maximum number of iterations is achieved. As the MSAA is stochastic, a predefined number of generations of runs is carried out to define the best solution.

The characteristics of the SSP damper used in [1] are analyzed to verify the proposed finite element modeling and the computation of the EDC (see Fig. 6), with L, R, and H being the damper's width, thickness, and height, respectively. E and X are the slot's width and the plate connection's thickness, respectively. In addition, the information would be used to generate a new set of initial solutions to verify the dependence of the optimized shape on the initial configuration. Finally, the performance of the proposed methodology is compared with those reported in the mentioned paper.

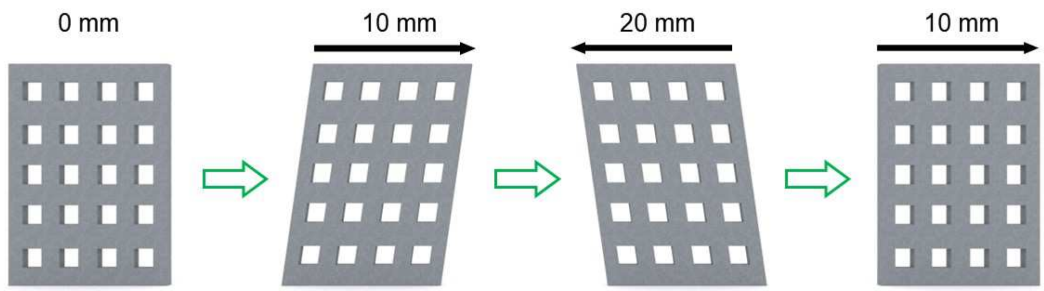

Fig. 5. Cyclic displacements for the loads.

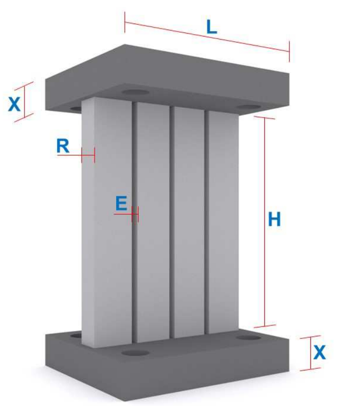

Fig. 6. Slotted Steel Plate Damper of reference proposed by Ghabraie et al. [2].

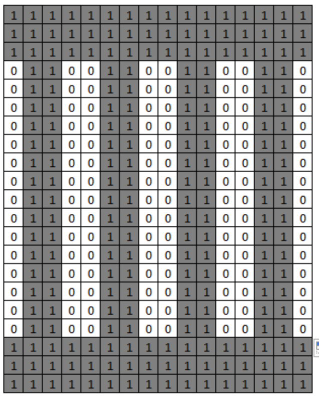

Fig. 7. Computational representation of a Rectangular steel plate. Value 0 represents a void, while value 1 represents a material point.

4.1 Formulation of the optimization problem

The mathematical formulation for any optimization problem in engineering requires the definition of four aspects: the design and parameters variables, the objective function, and the constraints on the search space. Consider a rectangular domain to define the optimal shape for the SSP damper, as shown in Fig. 6. The optimization algorithm determines which domain points correspond to material points to form the plate. Figure 7 presents a possible configuration for the SSP damper, where gray points correspond to material points. This issue can be computationally represented using a mesh of rectangular areas with values of 0 and 1 (Mz_01). The mesh size would equal the discretization of the finite element model. A value of 1 represents the presence of material in that area, and 0 is the opposite. Such representation presents three advantages, first from a computational point of view, second from mathematical operations and third from a visualization of the obtained shape. It is worth mentioning that applying a heuristic approach to an optimization problem depends on defining a "natural" representation of a possible solution.

The design parameters correspond to the characteristics of the SSP and modeling information that do not change during the optimization process. Those parameters include external space for the plate, material quantity, steel mechanical properties (elasticity modulus, yielding strength, Poisson coefficient, density, plastic stress, and deformation), and boundary conditions for the plate. The objective function corresponds to the maximization of the EDC computed from the stress on the plate domain that was obtained in the elastoplastic analysis carried out in Abaqus, as given by

$$Max\ F = EDC = \int f \times du \tag{4}$$

4.2 Simulated Annealing configuration

As the variable designs can only take values equal to 0 or 1, the modified SAA is forced to produce a trial that presents these values. After some tests, the results reported in this paper were obtained using the SAA parameters in Table 1. To achieve convergence, the performance criterion corresponds to a low standard deviation among runs and a lower number of iterations. Therefore, the trial solution is generated from the current one.

4.3 Proposed heuristic rules

Applying heuristics consists of using empirical rules to ease finding the solution to a problem, which is based on the knowledge of the problem to find high-quality solutions. The first heuristic for the study problem proposes accelerating the convergence process. The trial solution is modified according to the stress distribution obtained with Abaqus, see Fig. 8. The idea is to transfer the material with low stress to empty zones next to the material presenting high-stress values, increasing the effectivity of the mass distribution through the plate. The heuristic uses a change probability for each matrix position (i,j) in terms of the ratio between the stress, S, in the area and the maximum stress, Smax, in the plate, as given by Equation 5.

$$Pc_{ij} = \frac{S_{ij}}{S\max} \tag{5}$$

As seen, the points with higher stresses will have a lower probability of being changed. If the change probability for a one-value cell is lower than the mutation rate, its value will be 0. The next step consists of adjusting the exact quantities of cells with values equal to 0, as was changed before. Finally, the changing priority for a cell is computed based on the stresses of adjacent cells, as given by:

$$Po_{ij} = \frac{S_{(i-1,j)} + S_{(i+1,j)} + S_{(i,j-1)} + S_{(i,j+1)}}{4 \times S\max} \tag{6}$$

Table 1. SAA Parameters.

Parameters	Original SAA	Modified SAA
Population Size	1	5
Initial Temperature	1	0.70
Final Temperature	0.01	0.01
Cooling rate	0.70	0.80
Mutation rate	0.60	$0.60 \le Tm \le 0.85$
Maximum number of iterations	50	50
Number of runs	5	74.38

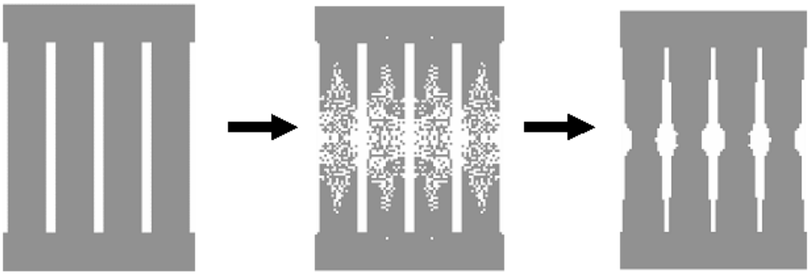

Fig. 8. Procedure to relocate material in the finite element model.

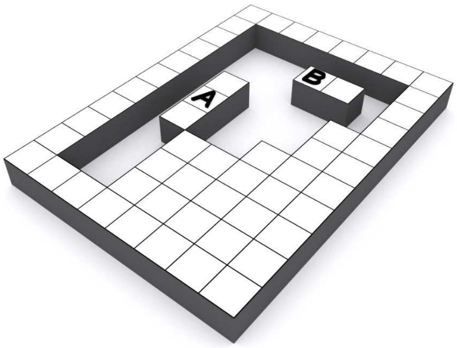

Fig. 9. Checkboard conditions [8].

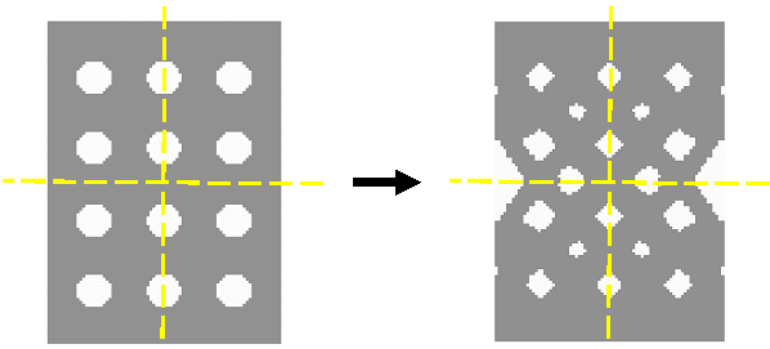

Fig. 10. Symmetry damper: (a) design solution and (b) trial solution keeping the symmetry.

The second heuristic is necessary to control the checkboard effect raised in two situations, see Fig. 9. The first relates to the fact that a trial solution can contain material cells with material that is not connected to any other material cells (point B). Also, only one node could join two material cells (point A), generating a problem with the finite element analysis. Therefore, to avoid such a situation, after the first heuristic is applied, each material cell (MZ_01) is assessed with Equation 7 to determine the cells with less than two orthogonal cells connected and requiring translation.

$$(Mz\_01_{(i-1,j)} + Mz\_01_{(i+1,j)} + Mz\_01_{(i,j-1)} + Mz\_01_{(i,j+1)}) < 2 \tag{7}$$

The third heuristic is defined to guarantee the double symmetry in the metallic damper. In that sense, the variable designs are reduced to one plate section, forcing the symmetry utilizing Equation 8. Figure 10 presents two examples of symmetries in plates.

$$Mz\_01_{(i,j)} = Mz\_01_{(-i-1,j)} = Mz\_01_{(i,-j-1)} = Mz\_01_{(-i-1,-j-1)} \tag{8}$$

4.4 Finite element model and computation of the energy dissipation capacity of the plate

ABAQUS was used to implement the finite element model that computes the SSP damper behavior under a cyclic excitation. In this case, the non-linear structural analysis is carried out in the plane, considering the S4R (4-node element for general use). Such consideration implies that the behavior through the thickness is uniform. The material selection depends on the steel employed for manufacturing, with the mechanical properties defined by a strain-stress curve obtained experimentally. Such a curve is introduced in ABAQUS, with the consideration of isotropic hardening as in [2]. It is worth mentioning that this research does not consider the effect of the steel type on the optimal configuration found. The boundary conditions correspond to fixed support on the lower side of the devices, while the upper side is only restricted to vertical movement. The cyclic displacement protocol is that illustrated in Fig. 5, with a series of displacement sub-steps. Further research could include the possibility of having a few cyclic displacements before the device's failure, as defined by chapter 18 of ASCE 7-16 [10].

Implementing a computational code in Python was necessary to couple with different parts related to the finite element modeling and the optimization process. The plastic dissipation energy is computed in the post-processing stage in ABAQUS. Further details can be observed in [17] regarding the automatic modeling process. Abaqus closes automatically after the main code sends the last instruction. Then, the main code extracts the analysis results in the Abaqus report, ending the communication process between Python and ABAQUS.

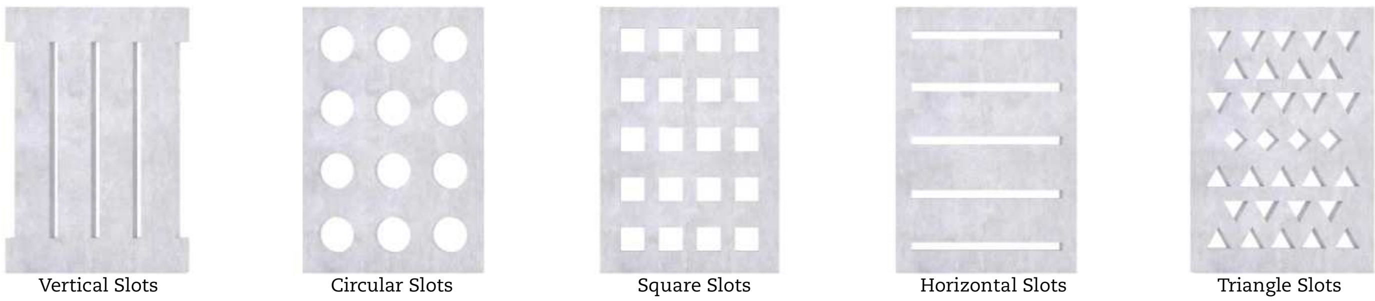

Fig. 11. Initial geometric shapes for the SSP dampers.

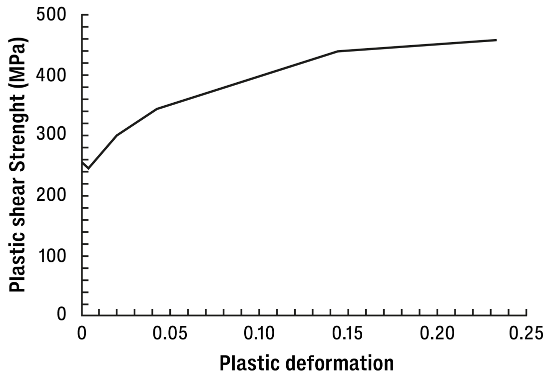

Fig. 12. Strain-stress curve for A-36 steel.

5. Numerical Examples

The proposed methodology is first used to optimize the vertical slot plate presented in Ghabraie et al. [2] with the aim of comparison. Then, the other four configurations are set up by modifying the shape of the slots, as shown in Fig. 11. The slot shapes correspond to simple geometric forms. All the plates present a search space of 140 mm in height, 100 mm in width, and 8 mm in thickness, a material area of 12000 mm^2, and a void area of 2000 mm^2 to produce a total material volume of 86000 mm^3. By testing different initial shapes, it is possible to determine their influence on the optimization process. The maximum size for the finite elements was 1.25mm, guaranteeing a correct assessment of the EDC and avoiding a high computational cost. It is necessary to make the finite element mesh for each analysis because each tested SSP configuration presents a different shape.

Concerning the mechanical parameters of the plate made of A-36 steel: density of 7.85 E-6 kg/mm3, modulus of elasticity of 210000 MPa, yielding strength of 250 MPa, and Poisson coefficient 0.30. The plastic properties are presented in the stress-deformation curve in Fig. 12, as introduced in ABAQUS. The SAA and MSAA determine the optimal configuration using the parameters in Table 1, considering five runs for each SSP damper in Fig. 11.

6. Results

6.1 Optimized Plates

Table 2 resumes the results obtained by applying the proposed methodology to the SSP initial configurations presented in Fig. 11, whose EDC is shown in Column 1. Again, the optimal EDC for each original and modified SAA run is reported, with the underlined value corresponding to the best EDC obtained for each SSP initial configuration. Results show that the best configuration for the plate has an EDC of 4609 J and that the difference with the worst configuration is 602 J (13% of the highest value). This result shows that the configuration chosen to start the search process has a moderated influence on the optimized EDC. It is worth noting that an initial configuration of the SSP damper with horizontal slots produces the optimal shape configuration despite presenting the lowest initial EDC. This finding implies that further analysis has to be carried out for an appropriate definition of the initial SSP configuration. The modified SSA was superior to the original but only created an optimized design with EDS higher in 116J (2.6 %) in most cases. Also, the highest difference of the EDC among runs is 427 J (10.8%), while that for the SAA is 325J (8.1%). This value shows that the modifications introduced on the SAA were lightly effective in increasing its performance for the problem in the study.

Table 2. Energy dissipation capacity for the optimized SSP dampers.

Slot shape	Type of SAA	Optimized energy dissipation capacity (J)					Best SAA
		1	2	3	4	5	
Circular 3054 J	Original	4102	4083	4033	4035	4092	Modified
	Modified	4158	3993	4191	4113	4141	
Square 2679 J	Original	4277	4344	4260	4217	4182	Modified
	Modified	4435	4460	4371	4443	4361	
Horizontal 1063 J	Original	4464	4602	4588	4584	4441	Modified
	Modified	4574	4599	4580	4609	4588	
Triangular 2864 J	Original	4356	4396	4298	4381	4262	Modified
	Modified	4458	4239	4174	4208	4309	
Vertical 1085 J	Original	3838	3682	4007	3779	3801	Original
	Modified	3548	3817	3966	3782	3539	

Table 3. Effect of the optimization process on the reshaping of the initial configuration.

Initial shape	Iteration N° 10	Iteration N° 20	Iteration N° 30	Iteration N° 40	Iteration N° 50
1085 J 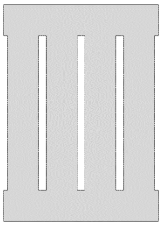	1789 J 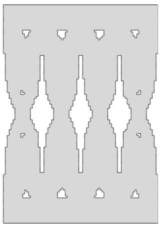	2605 J 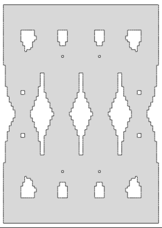	3347 J 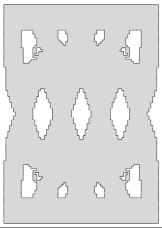	3512 J 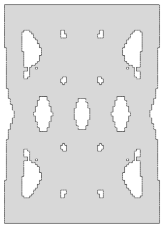	4007 J 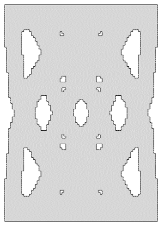
1063 J 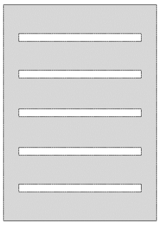	3094 J 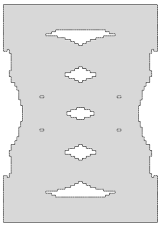	3913 J 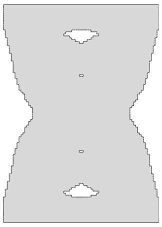	4377 J 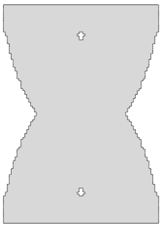	4233 J 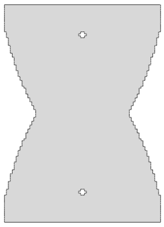	4609 J 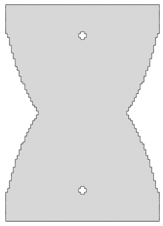

Table 4. Optimized shapes for plates.

Original Plate	Optimized Shape SAA	Smoothing SAA	Optimized Shape Modified SSA	Smoothing SAA	Improvement
3054 J 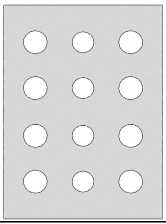	4102 J 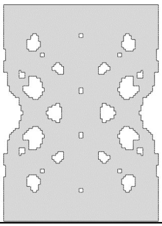	3984 J 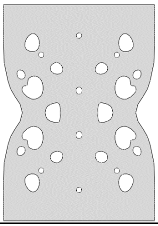	4191 J 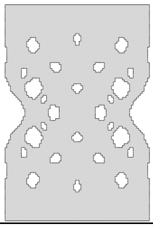	4099 J 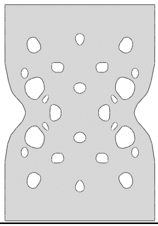	42.70%
2679 J 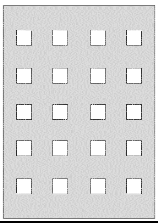	4344 J 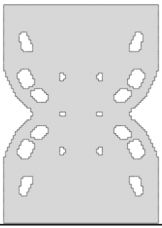	4099 J 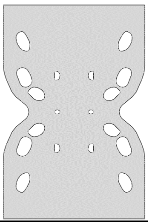	4460 J 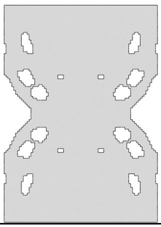	4313 J 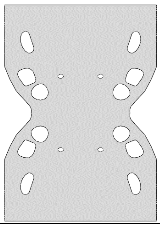	66.48%
1063 J 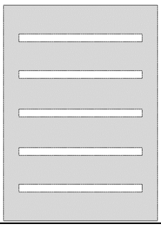	4602 J 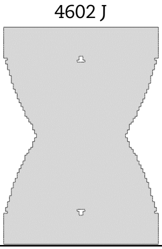	4612 J 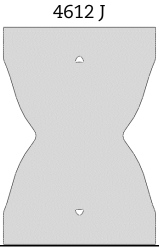	4609 J 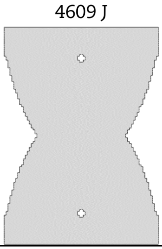	4591 J 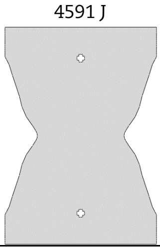	333.58%
2864 J 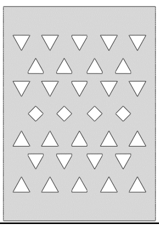	4396 J 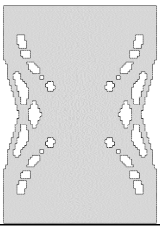	4062 J 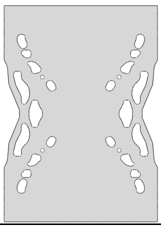	4458 J 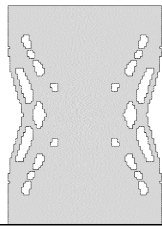	4277 J 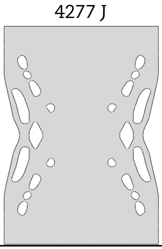	64.81%
1085 J 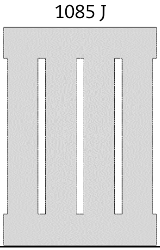	4007 J 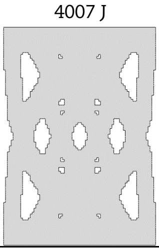	3780 J 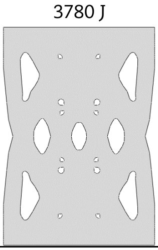	3966 J 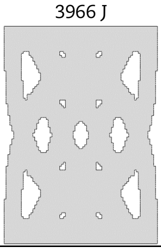	3778 J 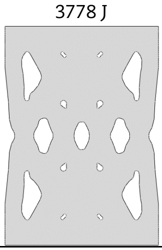	269.31%

One crucial issue that could improve the proposed methodology's performance is understanding how the optimization process reshapes the plate's initial configuration, increasing the EDC for the SSP damper. To illustrate this point, Table 3 presents the evolution of two initial configurations every ten iterations until producing the optimized shapes with the highest (Horizontal Slots) and lowest (vertical Slots) EDC. The process of convergence of the plate with horizontal slots was speedy. At iteration 10, it is observed that slots were mostly closed and the damper's center stretched, resulting in a device with 67% of the highest EDC of the optimal shape. At iteration 20, the EDC for the optimal solutions reached at least 85% of the best one, with only two significant slots kept. After that, the algorithm kept the plate's topology and improved its shape. However, a very different behavior was observed in the damper convergence process with vertical slots. The optimization tried to reshape the three vertical slots; however, it was slow until iteration 20, and only 65% of the final EDC had been achieved. Therefore, the process increased the number of slots to increase the EDC.

The optimized shapes obtained using the modified and original SAA for each initial plate are presented in Table 4. The highest increment was obtained in the horizontal slot configuration with four times the initial EDC, such a result was possible because the initial shape led the algorithm to lose the central slots and reshape the borders similarly to a sand clock shape. The lowest increment was obtained for the SSP configuration with triangular slots, with only a 64.81% improvement. In most cases, the topology changes considerably, trying to stretch the center of the plate. In addition, the initial shape influences the optimized shape as the modifications generated for the SAA are derived from that condition. Thus, it would be necessary to enlarge the initial configurations analyzed to determine other optimized shapes. One issue not studied in this research was the influence of the number of slots in the optimized shape.

On the other hand, applying a post-process of smoothing the shape obtained from the optimization process with the aim of fabrication is necessary. It is possible that the process generates non-smoothed solutions that would not be feasible to build as it does not consider manufacturing issues. In general, it was observed that this process produced a slight reduction in the EDC, except for the optimal shape with the honeycomb shape. It is worth mentioning that this configuration would be easily manufactured.

The computational time required for the finite element analysis of a plate, mesh 1.25 mm was 4 min 20s approximately; from this time, 1 minute is used to create the model and the other files. The total time for one run is 3 h 34 m for the SAA and 3 h 55 m for the modified SAA in a workstation with an Intel ® Xeon CPU of 2.20 GHz and 64 GB of RAM. One possibility for reducing the computational cost is employing population-based metaheuristics on parallel computers.

6.2 Stress States and Hysteresis Cycle for the Optimized Plates

Figures 13 to 17 (on the left) show the stress distribution for the initial and optimized plates. As observed, the initial configurations present high-stress values only around the slots' edge. The stress distribution through the plate is not uniform, and the maximum allowed value (485 MPa) is not reached, implying low EDC values. For the case of the best initial configuration with circular slots, it is observed that the stress is propagated from the edge of the plate to the external slots and then through to the intermedium vertical line of slots, with small areas lightly stressed. The ideal solution is obtained when the entire plate achieves the yielding for the cyclic displacement protocol. All the optimized models (Figs. 13 to 17 on the right) presented the maximum allowed value in most areas, with the remaining areas presenting at least 210 MPa. The distribution is uniformly distributed through the plate; this shows that the material is more effectively utilized. The optimal solution (Fig. 15) presents yielding zones clearly defined.

Figures 18 and 19 present the hysteresis cycles for the initial and optimized SSP configurations, considering the lowest and highest EDC devices. It can be observed that the area under the curve highly increases in both cases; therefore, its energy dissipation capacity also rises. The increment of highly concentrated stress areas in the optimized plates is related to the rise of the necessary force to obtain the same displacement quantity. The optimization process also increases the stiffness of the plate for all the initial configurations of the plates. Further studies should include the total EDC for several load cycles, including a possible deterioration in the hysteresis cycles.

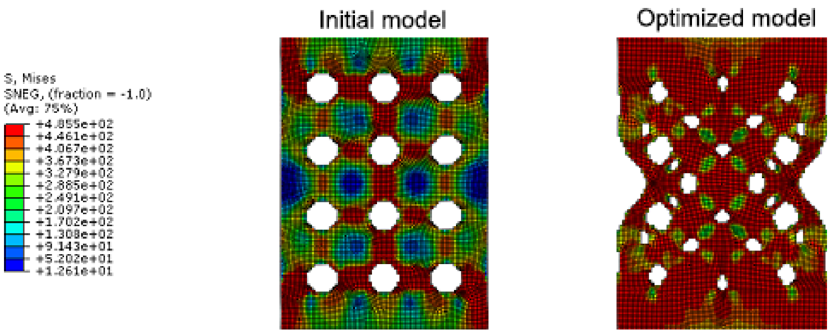

Fig. 13. Von-Mises Stress distribution for the plate with circular slots (on the left) and the optimized one (on the right).

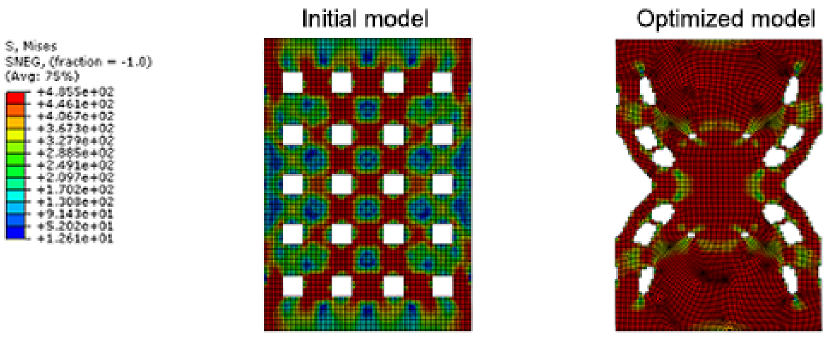

Fig. 14. Von-Mises Stress distribution for the plate with square slots (on the left) and the optimized one (on the right).

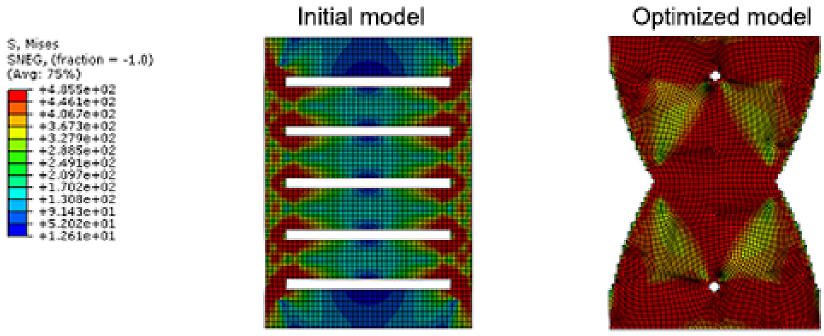

Fig. 15. Von-Mises Stress distribution for the plate with horizontal slots (on the left) and the optimized one (on the right).

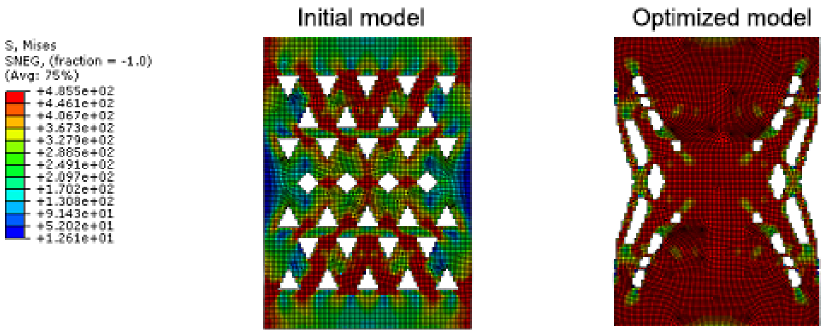

Fig. 16. Von-Mises Stress distribution for the plate with triangle slots (on the left) and the optimized one (on the right).

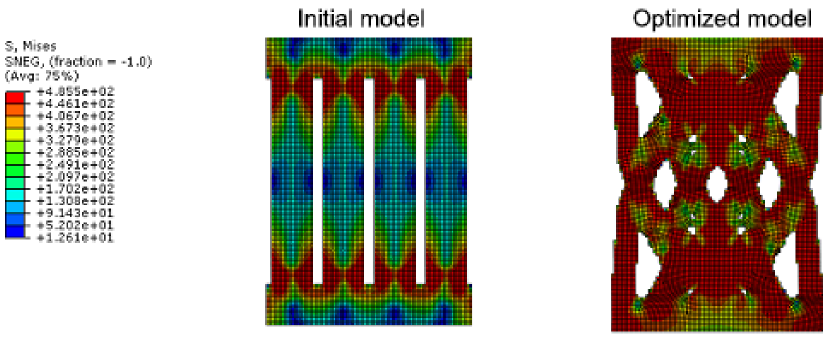

Fig. 17. Von-Mises Stress distribution for the plate with triangle slots (on the left) and the optimized one (on the right).

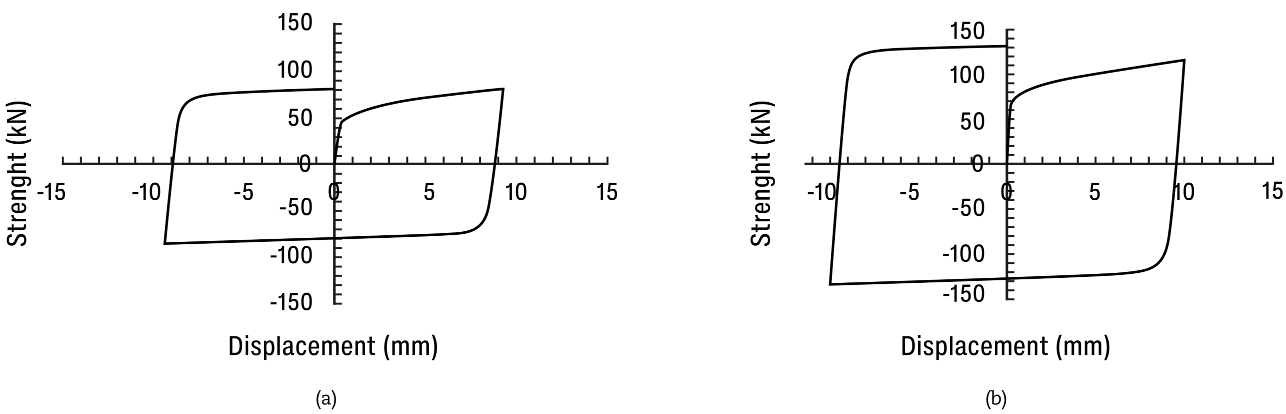

Fig. 18. Hysteresis cycles for the (a) initial and (b) optimized configuration: triangular slots.

6.3 Analysis of the Convergence of the Optimization Process

Figures 20 to 21 show the convergence process for the initial configuration plate with horizontal and vertical slots, considering the five runs. It is observed that the converging process is similar among runs for both SSA. Using 50 iterations was enough to guarantee the stabilization of the optimal solution. Generally, the SAA reaches convergence in the 25th iteration, ten iterations less than when the modified SAA is applied. However, fast convergence is not desired characteristic due to the likelihood of the algorithm getting stuck in a local optimum. Therefore, additional characteristics must be incorporated into the modified SAA to improve its ability to explore the search space in the final stage of the optimization process.

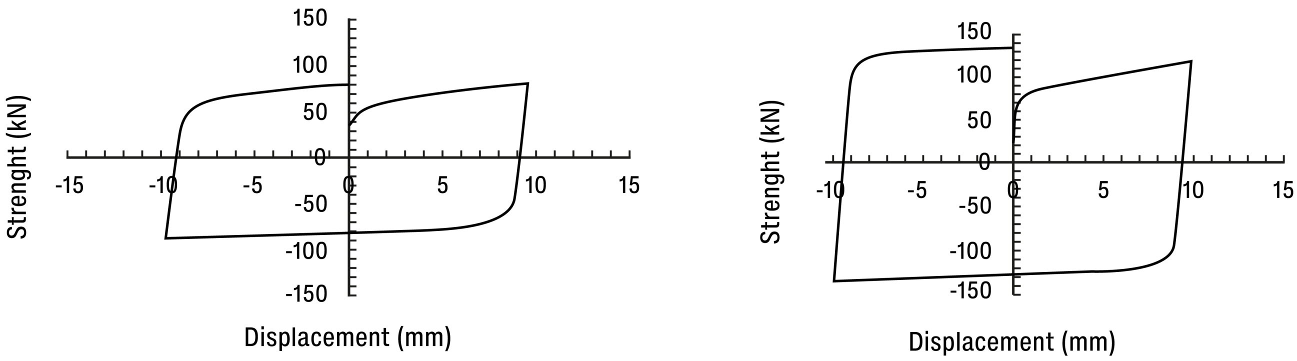

(a) (b)

Fig. 19. Hysteresis cycles for the initial and optimized configuration: horizontal slots.

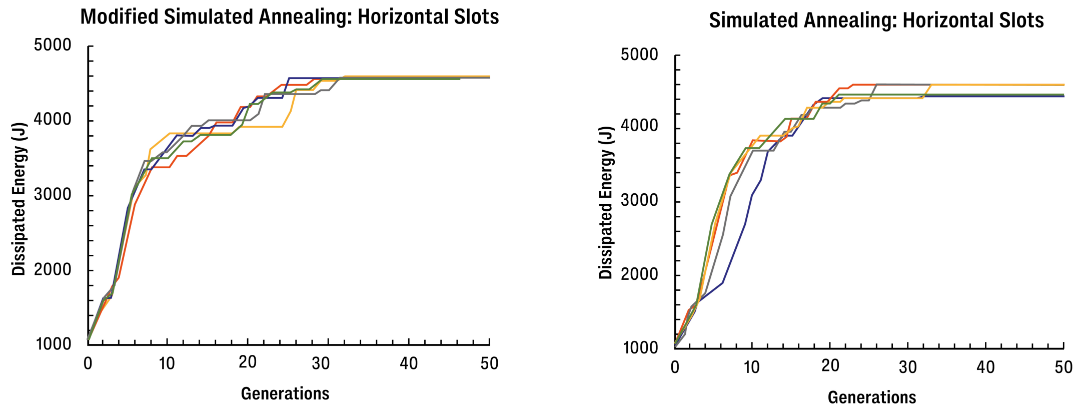

Fig. 20. Convergence results for the initial plate with horizontal slots.

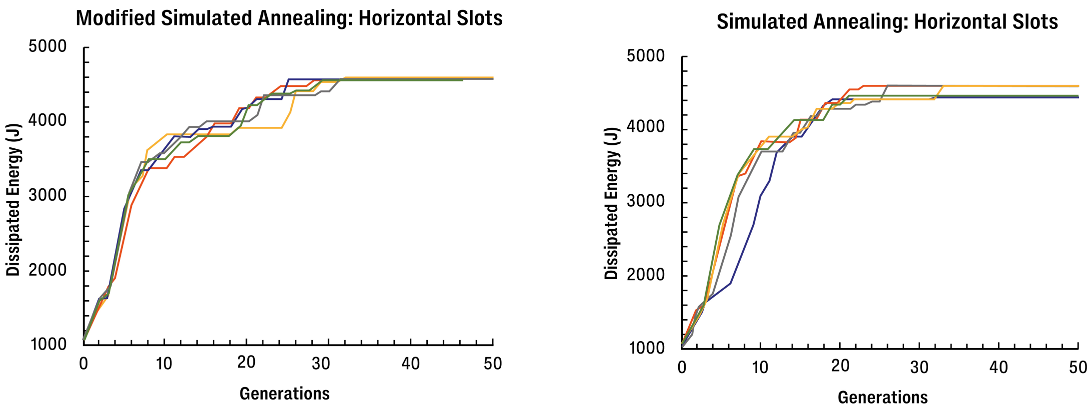

Fig. 21. Convergence results for the initial plate with horizontal slots.

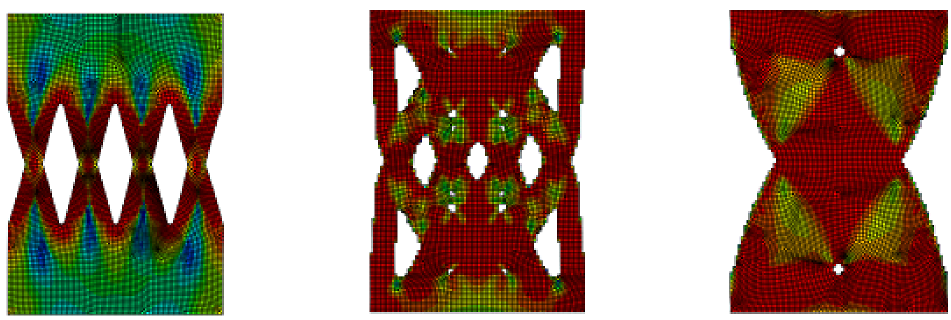

Optimized Configuration [2]: 2013 J   Optimized SSP 1: 4007 J   Optimized SSP 2: 4609 J

Fig. 22. Optimal shape and corresponding EDC in comparison with the results obtained in [1].

6.4 Verification of the results

The results for the SSP damper with vertical slots optimized by Ghabraie et al. [2] were used to compare. The initial Ghabraie's model generated presented an EDC of 1085J when reproduced in Abaqus, representing a slight difference from the reference model, whose EDC is 1124 J. This difference could be raised in modeling issues, but the result is acceptable. Then, the optimal shape found was compared with that obtained in Ghabraie's study, as shown in Fig. 22. As can be seen, the optimized form for the initial configuration with vertical slots has an EDC twice that obtained in [2]. This difference can be observed in the distribution of stresses in both plates. The plate obtained with MSAA has a higher area with the maximum allowed stress. The optimized solution found by Ghabraie et al. [2] is only 44% efficient compared with the optimal solution in this study.

7. Conclusions

The proposed metaheuristic procedure improves the design of slotted steel plate (SSP) dampers from initial geometric configurations with lower energy dissipation capacity (EDC). The process was validated from the computational implementation in python, establishing a communication process with ABAQUS, developing problem-knowledge heuristics, and implementing modifications to the optimization algorithm SAA to improve its performance. The main conclusions are summarized below:

- The computational difficulty for implementation is reduced by using a free-derivative algorithm such as SAA, which got converged in less than 50 iterations. Moreover, the computational interaction between ABAQUS and Python suits the problem.
- The modified SAA obtained better results in four of the five initial models than the original SAA, with varying levels lower than 5%. It was also possible to observe a better behavior of the modified SAA represented in a more extensive search space exploration.
- The generation of problem-knowledge heuristics for solving the problem is essential to converging the optimization process.
- The optimal solution presents an EDC of 4609 J, which represents an increment of 50.9% from the best initial SSP configuration and dissipates twice the energy of the optimal solution found in [2].
- For the tested initial slot configurations, the optimized solutions ranged with a minimum EDC of 4007J and a maximum of 4609J, reducing the initial difference in EDC from 64.47% to 13.06%. Thus, it is concluded that the search space is multi-modal.

This methodology is not limited to the examples this study gives; it can be used on plates of different sizes, masses, and materials. But the main restrictions are related to the fact that only one cycle is considered in the optimization process and that out-plane behavior is not considered. In addition, a different approach for handling the finite element model must be regarded to avoid the mesh.

Author Contributions

S. Ferrer-Fuenmayor and J.D. Villalba-Morales planned the scheme, initiated the project, and suggested the experiments. S. Ferrer-Fuenmayor implemented the proposed methodology computationally. The manuscript was written through the contribution of all authors. All authors discussed the results and reviewed and approved the final version of the manuscript.

Acknowledgments

Acknowledgments may be made to individuals or institutions that have made an important contribution.

Conflict of Interest

The authors declared no potential conflicts of interest concerning the research, authorship, and publication of this article.

Funding

The authors received no financial support for the research, authorship, and publication of this article.

Data Availability Statements

The datasets generated and/or analyzed during the current study are available from the corresponding author upon reasonable request.

Nomenclature

Δf	Difference between the quality of the trial and design solutions.	S_{ij}	Stress in the material point (i,j)
EDC	Energy Dissipation Capacity	Smax	Maximum Stress in the plate
f	Stress vector for the plate domain.	SSP	Slotted Steel Plate
Pc_{ij}	Probability of change for the position (i,j)	T	Temperature Parameter
SAA	Simulated Annealing Algorithm	u	displacement field

References

[1] Symans, M.D., et al. Energy dissipation systems for seismic applications: Current practice and recent developments, *Journal of Structural Engineering*, 134(1), 2008, 3-21.

[2] Ghabraie, K., Chan, R., Huang, X., Xie, Y., Shape optimization of metallic yielding devices for passive mitigation of seismic energy, *Engineering Structures*, 32, 2010, 2258-2267.

[3] Sahoo, D., Singhal, T., Taraithia, S., Saini, A., Cyclic behavior of shear-and-flexural yielding metallic dampers, *Journal of Constructional Steel Research*, 114, 2015, 247-257.

[4] Tai, K., Akhtar, S., Structural Topology Optimization Using a Genetic Algorithm with a Morphological geometric Representation, *Structural and Multidisciplinary Optimization*, 30, 2005, 113-127.

[5] Chan, R., Albermani, F., Kitipornchai, S., Experimental study of perforated yielding shear panel device for passive energy dissipation, *Journal of*

Constructional Steel Research, 91, 2013, 14-25.
[6] Hu, S., Wang, W., Qu, B., Seismic economic losses in mid-rise steel buildings with conventional and emerging lateral force resisting systems, *Engineering Structures*, 204, 2020, 110021.
[7] Sabelli, R., Mahin S., Chang, C. Seismic demands on steel braced frame buildings with buckling-restrained braces, *Engineering Structures*, 25, 2003, 655-666.
[8] Expósito, C., Melián, V., Moreno, J.M., A domain-specific knowledge-based heuristic for the Blocks Relocation Problem, *Advanced Engineering Informatics*, 28(4), 2014, 327-343.
[9] Deng, K., Peng, P., Sun, J., Liu, J., Xue, Y., Shape optimization design of steel shear panel dampers, *Journal of Constructional Steel Research*, 99, 2014, 198-193.
[10] American Society of Civil Engineers, *Minimum Design Loads and Associated Criteria for Buildings and Other Structures*, ASCE Press, 2016.
[11] Lee, C.H., Ju, Y.L., Min, J., Lho, S., Kim, S., Non-uniform steel strip dampers subjected to cyclic loadings, *Engineering Structures*, 99, 2015, 192-204.
[12] Li, H, Li, G, Li, Z, Xing, F., Earthquake-resistant design of reinforced concrete frame with metallic dampers of dual functions, *Journal of Building Structures*, 28(4), 2007, 36-43.
[13] Pimiento, J., Salas, A., Ruiz, D., Desempeño sísmico de un pórtico con disipadores de energía pasivos de placa ranuradas de acero, *Revista ingeniería de construcción*, 29(3), 2014, 283-298.
[14] Martinelli, E., Lima, C., Faella, C., Towards a rational strategy for seismic retrofitting of RC frames by combining member- and structure-level techniques, *Third Conference on Smart Monitoring, Assessment and Rehabilitation of Civil Structures*, Antalya, Turkey, 2015.
[15] Majid, T.A., Budiono, B., Experimental Study of Hysteretic Steel Damper for Energy Dissipation Capacity, *Advances in Civil Engineering*, 2015, 2015, 631726.
[16] Zheng, J., Li, A., Guo, T., Analytical and experimental study on mild steel dampers with non-uniform vertical slots, *Earthquake Engineering and Engineering Vibration*, 14, 2015, 111-1223.
[17] Ferrer-Fuenmayor, S., Villalba-Morales, J., Numerical assessment of dissipation energy capacity in perforated plate steel dampers, *Dyna*, 88(218), 2021, 194-202.
[18] Xu, Y.H., Li, A.Q., Zhou, X.D., Sun, P., Shape Optimization Study of Mild Steel Slot Dampers, *Advanced Materials Research*, 168-170, 2010, 2434-2438.
[19] Watanabe, H., Ohsaki, M., Nozoe, J., Yasuda S., Shape Optimization of Shear-type Hysteretic Steel Damper for Building Frames using FEM-Analysis and Heuristic Approach, *The Seventh China-Japan-Korea Joint Symposium on Optimization of Structural and Mechanical Systems*, Huangshan, China, 2012.
[20] Liu, Y., Shimoda, M., Shape optimization of shear panel damper for improving the deformation ability under cyclic loading, *Structural and Multidisciplinary Optimization*, 48, 2013, 427-435.
[21] Zhu, B.J., Wang, T., Zhang, L.X., Mechanical behavior of assembled steel dampers with optimized shapes, *Key Engineering Materials*, 763, 2018, 956-966.
[22] Farzampour, A., Khatibinia, M., Mansouri I., Shape optimization of butterfly-shaped shear links using grey wolf algorithm, *Civil and Environmental Engineering*, 2019.
[23] Deng K., Pan, P., Li, W., Xue, Y., Development of a buckling restrained shear panel damper, *Journal of Constructional Steel Research*, 106, 2015, 311-321.
[24] Oviedo, J., Midorikawa, M., Asari, T., Earthquake response of ten-story story-drift-controlled reinforced concrete frames with hysteretic dampers, *Engineering Structures*, 32(6), 2010, 1735-1746.
[25] Yongjiu, S., Meng, W., Yuanqing, W., Experimental and constitutive model study of structural steel under cyclic loading, *Journal of Constructional Steel Research,* 67(8), 2011, 1185-1197.
[26] Wang, M., Fahnestock, L., Qian, F., Yang, W., Experimental cyclic behavior and constitutive modeling of low yield point steels, *Construction and Building Materials,* 131, 2017, 696-712.
[27] Jie, Z., Li, A., Guo, T., Analytical and experimental study on mild steel dampers with non-uniform vertical slots, *Earthquake Engineering & Engineering Vibration,* 14, 2015, 111-123.
[28] Perri, F., Faella, C., Martinelli, E., Cost-competitive hysteretic devices for seismic energy dissipation in steel bracings: experimental tests and low-cycle fatigue characterization, *Construction and Building Materials,* 113, 2016, 57-67.
[29] Bae, J., et al., Modified Low-Cycle Fatigue Estimation Using Machine Learning for Radius-Cut Coke-Shaped Metallic Damper Subjected to Cyclic Loading, *International Journal of Steel Structures,* 20(6), 2020, 1849-1858.
[30] Shi, G., Gao, Y., Wang, X., Zhang, Y., Mechanical properties and constitutive models of low yield point steels, *Construction and Building Materials*, 175, 2018, 570-587.
[31] Javanmardi, A., Ibrahim, Z., Ghaedi, K., Benisi Ghadim, H., Hanif, M., State-of-the-Art Review of Metallic Dampers: Testing, Development and Implementation, *Archives of Computational Methods in Engineering*, 27(2), 2019, 455-478.
[32] Kirkpatrick, D., Gelatt, C.D., Vecchi, M.P., Optimization by Simulated Annealing, *Science,* 220(4598), 1983, 671-380.
[33] Millan, C., Begambre, O., Solución de problemas de optimización topológica empleando el algoritmo Simulated Annealing modificado, *Revista Internacional de Métodos Numéricos para Cálculo y Diseño en Ingeniería*, 32(2), 2016, 65-69.
[34] He, R.S., Hwang, S.F., Damage detection by an adaptive real-parameter simulated annealing genetic algorithm, *Computers & Structures*, 84(31-32), 2006, 2231-2243.
[35] Hasancebi, O., Carbas, S., Saka, M.P., Improving the Performance of Simulated Annealing in Large-Scale Structural Optimization, *Structural and Multidisciplinary Optimization*, 41(2), 2010, 189-203.
[36] Aydin, A., Simple damper optimization algorithm for both targets added damping ratio and interstory drift ratio, *Earthquakes and Structures*, 5(1), 2013, 083-109.
[37] Tong, K.H., Bakhary, N., Kueh, A.B.H., Mohd Yassin, A.Y., Optimal sensor placement for mode shapes using improved simulated annealing, *Smart Structures and Systems*, 13(3), 2014, 389-406.

ORCID iD

Samuel Ferrer-Fuenmayor https://orcid.org/0000-0002-4521-3291
Jesús D. Villalba-Morales https://orcid.org/0000-0001-8339-2262

How to cite this article: Ferrer-Fuenmayor S., Villalba-Morales J.D. Shape Optimization of Slotted Steel Plate Dampers using the Simulated Annealing Algorithm, *J. Appl. Comput. Mech.*, 9(3), 2023, 870–883. https://doi.org/10.22055/jacm.2023.42249.3895